"Helium Spots": Caused by a Diapiric Magma from the Upper Mantle

Abstract. *"Helium spots," where a significant amount of helium is present in the soil [up to 350 parts per million with a high ^3He to ^4He ratio of $(8.90 \pm 0.31) \times 10^{-6}$], have been found along the fault zone formed by the 1966 Matsushiro swarm earthquakes. The formation of the "helium spots" and the occurrence of the earthquakes are interpreted as the results of a diapiric uprise of a magma approximately 1 kilometer in diameter.*

Measurements of variations in the degassing rate from a fault can be a good way of inferring the most recent time of displacement along a fault, including displacements such as creep and stick slip. Helium is thought to be one of the most ideal elements to measure for this purpose because of its mobility, chemical inertness, and low abundance in the atmosphere. By means of such a geochemical tracer, we aimed at a qualitative assessment of an active fault related to the occurrence of an earthquake. Helium surveys have already been attempted for prospecting for natural gases, ores, and active geothermal areas (*1*). Application of a similar technique to active fault zones may provide useful information for earthquake prediction and also for the assessment of the helium budget for the earth-atmosphere system.

A series of field experiments has been done in the Matsushiro area for 2½ years, starting in November 1975. Measurements of helium concentration have been conducted on soil collected along the fault zone formed by the Matsushiro swarm earthquakes. The Matsushiro earthquakes occurred during the period 1965 to 1967, at and around Matsushiro in central Japan (Fig. 1). In the most active period, more than 600 felt earthquakes occurred in one day. The maximum magnitude of the earthquakes was 5.3 on the Richter scale and the total energy released was equivalent to that of a single earthquake of magnitude 6.3. The earthquake foci, within an area about 4 km in diameter, were centered beneath the Minakamiyama andesitic dome, and spread gradually in a northeast to southwest direction. Initially the depths of the foci were about 4 to 5 km, but they showed a tendency to move upward with the progression of seismic activities (*2*). A left-lateral fault with a northwest to southeast strike was formed during the same period. Various abnormal phenomena, including changes in gravity, magnetic field and ground upheaval, tilting, groundwater gushing, and electric lightning were also observed. There have been many intensive studies on the Matsushiro earthquake swarm (*3*) and various attempts to explain the processes of the swarm (*4, 5*).

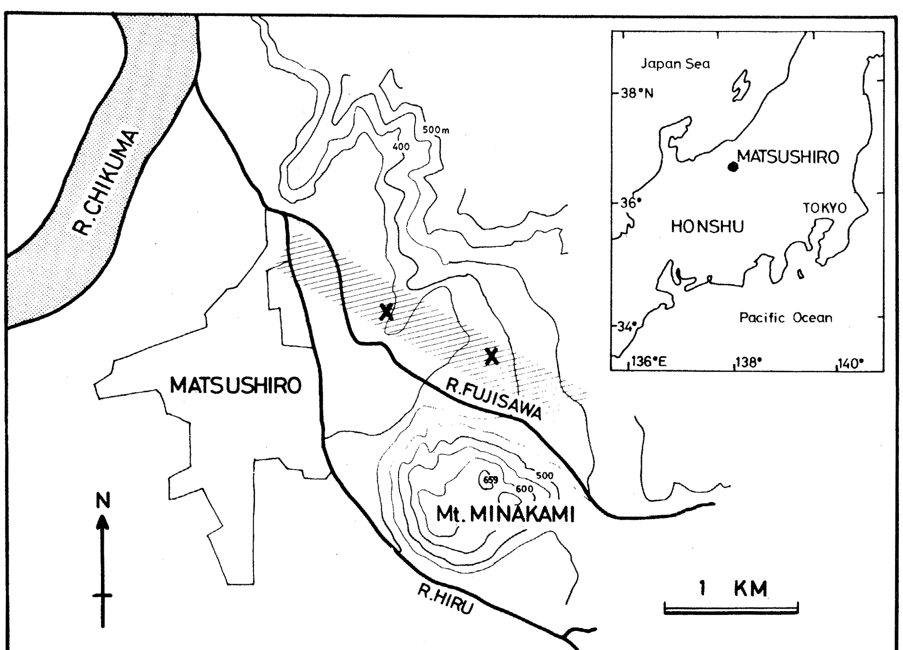

Fig. 1. Map showing the Matsushiro area and "helium spots" (X). Ruled area is a fault zone associated with the 1966 Matsushiro earthquakes.

The most peculiar phenomenon associated with the earthquake swarm was the gushing of a significant amount of groundwater, which was characterized by an anomalous chemical composition. The locus of groundwater gushing coincided with the northwest to southeast fault zone and was confined to an area about 5 km in length and 1 km in width. It was estimated that a total of 10^7 m^3 of groundwater was released from about 70 sites in the area. The estimated flow rate of 12 m^3/min was recorded at one site in the fall of 1966 (*6*). The gushing of the groundwater occurred when the uplifted surface started to subside, and the estimated volume of water was close to the volumetric shrinking during subsidence (*4*). Changes in the flow rate and chemical composition of hot spring water of a shallower origin were also reported. The surface water of the area was different in chemical composition from the gushed groundwater. The surface water contained chlorine and calcium ions at concentrations of thousands of parts per million and was supersaturated with carbon dioxide (*7, 8*). As seismic activity progressed, changes in the ratio of Ca to Cl of hot spring water were noted (*7*). Several CO_2 springs were formed during that period. Concurrently with the decrease in the gushing rate of groundwater, seismic activities also declined, indicating that the gushing of groundwater may have played an important role in the occurrence of the earthquakes. Although there are no significant quakes at the present time, groundwater seepage has continued on a small scale within the fault zone.

Among the various gas collecting methods available, we adopted the displacement method (method of substituting gas over an aqueous phase) for this project (*9*). After a certain period of storage time, either some of the collected soil-gas samples were introduced into a mass spectrometer (a helium leak detector, model DLMS-33, ULVAC, Japan) through a sniffer probe, or two sets of gas chromatograph were used: one for He, Ar, N_2, and CH_4 analyses and the other for CO_2 analysis. The detection limits of helium measurements were about 0.1 and 10 ppm for the mass spectrometer and the gas chromatograph, respectively.

In the fault zone, the helium concentration in the soil gas was higher than the normal atmospheric concentration (5.2 ppm), but that of the soil gas from outside the fault zone was the same as that

0036-8075/78/0428-0430$00.50/0

in the atmosphere. The highest concentration measured so far was about 350 ppm. Helium degassing was not homogeneous throughout the fault zone but was unevenly distributed in "helium spots" with approximate areas of 50 by 30 m.

During the rice grass planting season, water is introduced into the rice fields and gas bubbles containing helium from small vents are easily visible. The number of vents per helium spot was estimated to be about 200 to 300. By means of the displacement method mentioned above, the flow rate, chemical composition, and helium concentration of the released gas were measured. The flow rate of the bubbling gas for the active vents and for ordinary vents averaged about 100 ml/min and 10 ml/min, respectively. The gas consisted mostly of N_2 with about 20 percent CO_2. The gas obtained from a CO_2 spring situated nearby had a composition of approximately 93 percent CO_2 and 7 percent N_2. The helium concentrations of these two types of gas were significantly different. In the N_2-rich gas the He concentration was as much as 350 ppm, while in the CO_2-rich gas the He concentration was about 5 ppm.

Several methods of estimating the helium flux for a "helium spot" with an area of approximately 30 by 50 m were attempted. Since the estimated flow rate of the released gas from this particular area is about 50 ml/sec and the helium concentration of it is 350 ppm, the helium flux is about 3×10^{10} atom cm^{-2} sec^{-1}. This value is much higher than the average crustal production rate of helium, which is 10^6 atom cm^{-2} sec^{-1} (*10*).

With regard to the origin of the high helium flux in the Matsushiro area, it is known that the helium flux is high in areas where uranium ores, oil fields, and gas deposits occur. However, no sign of such deposits beneath the Matsushiro district has been found.

Unusually high $^3He/^4He$ isotope ratios, $(8.90 \pm 0.31) \times 10^{-6}$ and $(8.87 \pm 0.55) \times 10^{-6}$, were obtained for the gas from "helium spots" and CO_2 springs, respectively. These ratios are six times higher than the atmospheric ratio but are similar to those of volcanic gases and hot springs from the Kurile Islands (*11*) and of ultramafic xenoliths of mantle origin from Kamchatka and Antarctica (*12*). By means of a stepwise heating method, Tolstikhin *et al.* found high $^3He/^4He$ ratios only in the fractions extracted from xenoliths at temperatures higher than 1000°C. Evidence of injection of primordial helium from the mantle has also been reported for glassy rims of tholeiites from the Atlantic and Pacific rises (*13, 14*), for fumaroic gases from Kilauea volcano (*14*), and for brines from the Red Sea (*15*).

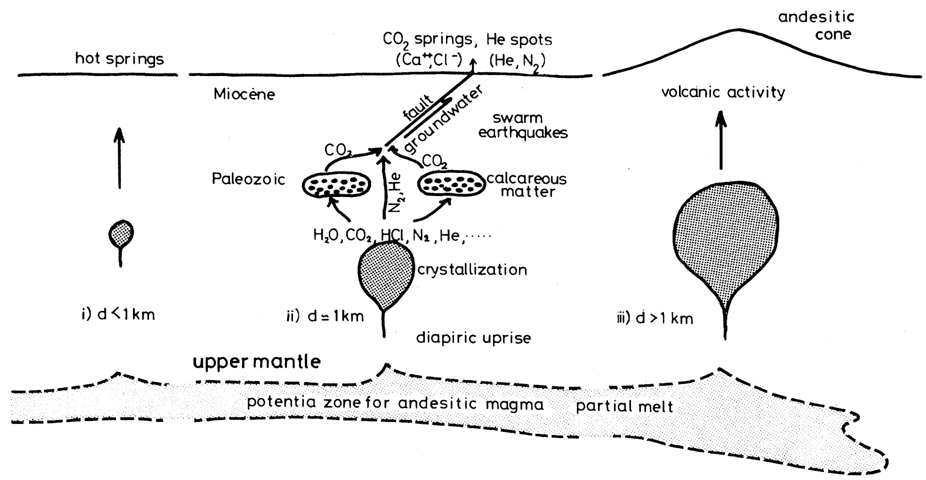

Fig. 2. Schematic diagram of diapiric uprise of a magma that originated in the upper mantle, and subsequent formation of "helium spots." Different volumes of the original roughly spherical diapir would result in different phenomena: (i) for diameter (d) less than 1 km, the result would be local geothermal effects; (ii) for $d \simeq 1$ km, earthquake swarms; and (iii) for $d > 1$ km, volcanic activity.

We postulate that the helium source is related to the cause of the Matsushiro earthquakes. The high helium degassing rate observed in this area appears to be closely related both in time and space to the swarm of earthquakes. Other associated phenomena, such as ground upheaval, gravity changes, faulting, and gushing of groundwater may be somehow related to the "helium spots."

The most plausible cause of these phenomena would be a small, shallow magmatic intrusion. A small mass of magma, about 1 km in diameter (*16*), which separated from a source in the upper mantle, may have risen diapiricly. As the temperature of the rising magma declines, crystallization of an andesitic rock begins, and volatile materials in the melt, such as H_2O, HCl, CO_2, N_2, and He, are excluded. Because this degassing process takes place for short periods of time, the supposed diapir may actually consist of a number of small bodies. Ascending magmatic fluids, mixed with the local groundwater, increase the pore pressure, and decrease the effective stress of the layer in the upper crust, in a preexisting tectonic stress field. This results in numerous earthquakes. Groundwater flows to the ground surface through faults (*17*). On its way upward, hydrochloric acid from the magma attacks calcareous matter, such as limestones in the Paleozoic strata that probably underlie the area. These dissolved components add high concentrations of Ca ions, Cl ions, and CO_2, with a $\delta^{13}C_{PDB}$ (*18*) of $-1 \sim -3$. The newly formed CO_2 dilutes the original gas composition to the point where it may form a CO_2 spring. Through another path to the ground surface, free from calcareous material, the original composition could be better preserved and would form a "helium spot" (Fig. 2).

When the volume of the diapiric magma is small, less than 1 km in diameter, it would yield only local geothermal effects, such as hot springs. On the other hand, if the volume is sufficiently large (that is, larger than 1 km in diameter), volcanic eruptions would result. The suggested diameter of 1 km for a diapiric magma seems to be suitable for occurrence of earthquake swarms.

HIROSHI WAKITA
Department of Chemistry, University of Tokyo, Tokyo 113, Japan
NAOYUKI FUJII*
Geophysical Institute, University of Tokyo
SADAO MATSUO
Department of Chemistry, Tokyo Institute of Technology, Tokyo 152
KENJI NOTSU
Department of Chemistry, Tsukuba University, Ibaragi 300-31, Japan
KEISUKE NAGAO
NOBUO TAKAOKA
Department of Physics, Osaka University, Toyonaka, Osaka 560, Japan

References and Notes

1. A. A. Roberts, I. Friedman, T. J. Donovan, E. H. Denton, *Geophys. Res. Lett.* **2**, 209 (1975); W. Dyck, *J. Geochem. Explor.* **5**, 3 (1976).
2. M. Ohtake and K. Hamada, *Zisin, J. Seism. Soc. Jpn.* **28**, 321 (1975).
3. See, for example, *Earthq. Res. Inst. Bull. Univ. Tokyo* **44**, 307 (1966); *ibid.* **45**, 159 (1967); *ibid.* **46**, 417 and 485 (1968).
4. K. Nakamura, *Kagaku Asahi, No. 10* (1971), p. 127; C. Kisslinger, *Geology* **3**, 57 (1975).

5. A. Nur, *Geology* **2**, 217 (1974); W. D. Stuart and M. J. S. Johnston, *ibid.* **3**, 63 (1975); M. Ohtake, *Kagaku* **46**, 306 (1976).
6. H. Iijima, *Report Cooperative Research Disaster Prevention No. 18* (National Research Center for Disaster Prevention, Tokyo, 1969), p. 103.
7. K. Noguchi, S. Ueno, T. Nishido, *Onsen Kagaku* **20**, 67 (1969).
8. R. Yoshioka, S. Okuda, Y. Kitano, *Geochem. J.* **4**, 61 (1970).
9. Holes with depths of 40 to 220 cm were drilled by a soil auger. A funnel with a stopcock attached was placed over the hole and sealed with bentonite. Trays 50 by 50 by 2 cm also covered the ground surface. A detailed description of the collection of soil gas and measurement and calibration techniques for the mass spectrometer and gas chromatographs will be published elsewhere.
10. G. Kockarts, *Space Sci. Rev.* **14**, 723 (1973).
11. I. L. Kamenskiy, V. P. Yakutseni, B. A. Mamyrin, S. G. Anufriyev, I. N. Tolstikhin, *Geochem. Int.* **8**, 575 (1971).
12. I. N. Tolstikhin, B. A. Mamyrin, L. B. Khabarin, E. N. Erlikh, *Earth Planet. Sci. Lett.* **22**, 75 (1974).
13. J. E. Lupton and H. Craig, *ibid.* **26**, 133 (1975).
14. H. Craig and J. E. Lupton, *ibid.* **31**, 369 (1976).
15. J. E. Lupton, R. F. Weiss, H. Craig, *Nature (London)* **266**, 244 (1977).
16. When a magma of volume 5×10^8 m^3 (equivalent to that of a spherical body 1 km in diameter) contains 2 percent water by volume, the total amount of water is 10^7 m^3.
17. H. Mizutani and T. Ishido, *J. Geomagn. Geoelectr.* **28**, 179 (1976). The magnetic field variation associated with the Matsushiro earthquakes has been interpreted as caused by the electrokinetic effect induced by water diffusion.
18. $\delta^{13}C_{PDB} = \{(^{13}C/^{12}C)_{sample} - (^{13}C/^{12}C)_{PDB}\}/(^{13}C/^{12}C)_{PDB} \times 1000$ where PDB refers to Pee Dee belemnite, the international standard of carbon isotope ratio.

19. We thank T. Asada, M. Ozima, and J. T. Iiyama for advice and encouragement in this study; K. Nakamura and A. McBirney for reading the manuscript and for criticism; and T. Yamada for field assistance. Supported in part by the Ministry of Education.

* Present address: Department of Earth Sciences, Kobe University, Kobe 657, Japan.

28 November 1977; revised 24 January 1978

Rifampicin Inhibition of Protein Synthesis in Mammalian Cells

Abstract. *Rifampicin produces a dose-dependent decrease in protein synthesis in rat thymocytes. At concentrations up to 200 micrograms per milliliter, rifampicin does not alter rat thymic transcription. Rifampicin causes a direct inhibition of protein synthesis in rat thymic and hepatic microsomes, and in cadaveric human hepatic microsomes. Protein synthesis inhibition could explain the toxicity of rifampicin in man.*

The rifamycin antibodies have become important therapeutic agents since their isolation in 1959 (*1, 2*). Rifamycin binding to the β subunit of bacterial RNA polymerase results in the inhibition of transcription initiation (*3*). In contrast, eukaryotic transcription is not affected by rifampicin until much higher concentrations are attained (*4*). Clinical treatment of tuberculosis with rifampicin requires the oral administration of 300 to 600 mg/day (*5*). Oral administration of 600 mg of rifampicin per day to seven patients for 4 months resulted in mean peak serum concentrations of 7 μg/ml, whereas serum concentrations after a single 450-mg dose ranged up to 28 μg/ml (*1*). Organs such as the kidney, liver, and lung contained higher rifampicin concentrations than serum. After a single rifampicin dose of 450 mg, the liver contained 36 μg/g and bile 538 μg/ml (*1*).

Long-term administration of rifampicin has been shown to shorten the biological half-life of anticoagulants, glucocorticoids, oral contraceptives, and rifampicin itself, presumably through induced alterations in heptic metabolism (*6*). Rifampicin may induce abnormalities in heptic function, a toxic effect which may progress to necrosis (*5, 7*). Rifampicin is also immunosuppressive. In animals and in man, rifampicin inhibits both in vivo and in vitro humoral and cellular immunological responses (*8–10*). In man, rifampicin reduces lymphocyte proliferative responses in vivo to phytohemagglutinin and purified protein derivative (*9, 11*). Rifampicin applied locally to smallpox vaccination sites impaired the production of antibody (*12*). The formation of T lymphocyte rosettes and the response of humoral antibody to keyhole limpet hemocyanin were reduced in patients receiving rifampicin (*10, 13*).

In this report we demonstrate the effects of rifampicin on macromolecular synthesis in rat thymocyte suspensions in vitro. The most pronounced effect of rifampicin is a dose-dependent decrease in protein synthesis that begins at concentrations achieved in the serum of humans being treated with rifampicin. Protein synthesis is inhibited in the presence of increases in the specific activity of the soluble amino acid pool. Inhibition of protein synthesis by rifampicin is directly demonstrable in subcellular microsomal fractions from rat thymocytes and hepatocytes, and cadaveric human hepatocytes.

Male Simonsen Sprague-Dawley rats (60 to 100 g) were decapitated and their thymus glands excised, weighed, and minced in cold buffer containing 5.5 mM glucose, 5.0 mM KCl, 1.0 mM $MgSO_4$, 5.0 mM Na_2HPO_4, 120.0 mM NaCl, 5.0 mM tris, and 1.0 mM $CaCl_2$, adjusted to pH 7.2 at 25°C (*14*). Minced thymic tissue (0.05 g of thymus per milliliter of buffer) was transferred to a Dounce homogenizer and a cell suspension prepared with three strokes of a loose-fitting pestle. Cell suspensions were filtered, counted with a hemacytometer, and diluted to 170,000 thymocytes per milliliter of buffer. Thymocytes were then incubated with and without rifampicin under conditions which measured macromolecular synthesis. Rifampicin (500 μg/ml) was dissolved in buffer by stirring overnight at 2°C.

Rifampicin induced dose-dependent decreases in [^{3}H]thymidine, [^{3}H]uridine, and L-[^{3}H]leucine incorporation (Fig. 1). Similar decreases in protein precursor incorporation occurred when proteins were labeled with mixed ^{3}H-labeled L-amino acids in place of L-[^{3}H]leucine. The specific activity of the amino acid pool increases as the rifampicin concentration is increased (see Fig. 2). The data in Figs. 1 and 2 suggest that rifampicin inhibits protein synthesis in mammalian

Table 1. Effect of rifampicin on thymocyte transcription. Assays for RNA polymerase activity were performed according to Chamberlin and Berg (*20*) as modified by Roeder and Rutter (*21*). The assay medium contained 10 μmole of tris (pH 7.9), 0.5 μmole of 2-mercaptoethanol, 1.0 μmole of $MgCl_2$, 0.5 μmole of $MnCl_2$, 0.1 μmole of ATP, cytidine triphosphate (CTP), and GTP, and 0.01 μmole of uridine triphosphate (UTP). Tenfold increases or decreases in UTP concentration at constant specific activity indicated that the UTP concentration was not limiting. Calf thymus DNA was added in four- to fivefold excess (50 μg), then crude nuclear extract containing RNA polymerase was added to give a total of 150 μg of protein. The added nuclear extract containing RNA polymerase activity resulted in a final glycerol concentration of 3 to 5 percent. Maximum incorporations [expressed as disintegrations per minute (dpm) per assay] were determined in the presence and absence of rifampicin by adding 5 μCi of [5-^{3}H]uridine-5′-triphosphate (24 Ci/mmole) to initiate 15-minute periods of incubation at 37°C. Maximum incorporations were equal to incorporation rates at 8 minutes, after which incorporation plateaued unless higher glycerol concentrations were used (*22*). Transcription was terminated by the addition of cold $Na_4P_2O_7$ (100 μmole/ml) containing BSA (1 mg/ml), followed by 12 percent TCA. Precipitated material was collected by centrifugation at 17,300g_{max} for 10 minutes. Pellets were washed twice by dissolving in NaOH, then reprecipitated and prepared for counting as described for thymocytes (Fig. 1). Values shown are means (± standard error) of six replicates. All values are corrected for background counts and for color quenching. Average counting efficiency was 30 percent.

Rifampicin (μg/ml)	[^{3}H]UMP incorporation (dpm/assay)	
	Experiment 1	Experiment 2
0	1070 ± 48	1310 ± 70
20	1099 ± 60	1344 ± 70
200	1000 ± 128	1173 ± 117